



**HAL**  
open science

## Inter-comparison of stable iron, copper and zinc isotopic compositions in six reference materials of biological origin

Lucie Sauzéat, Marta Costas-Rodríguez, Emmanuelle Albalat, Nadine Mattielli, Frank Vanhaecke, Vincent Balter

### ► To cite this version:

Lucie Sauzéat, Marta Costas-Rodríguez, Emmanuelle Albalat, Nadine Mattielli, Frank Vanhaecke, et al.. Inter-comparison of stable iron, copper and zinc isotopic compositions in six reference materials of biological origin. *Talanta*, 2021, 221 (6), pp.121576. 10.1016/j.talanta.2020.121576 . hal-03903489

**HAL Id: hal-03903489**

**<https://uca.hal.science/hal-03903489v1>**

Submitted on 16 Dec 2022

**HAL** is a multi-disciplinary open access archive for the deposit and dissemination of scientific research documents, whether they are published or not. The documents may come from teaching and research institutions in France or abroad, or from public or private research centers.

L'archive ouverte pluridisciplinaire **HAL**, est destinée au dépôt et à la diffusion de documents scientifiques de niveau recherche, publiés ou non, émanant des établissements d'enseignement et de recherche français ou étrangers, des laboratoires publics ou privés.



Distributed under a Creative Commons Attribution - NonCommercial - NoDerivatives 4.0 International License

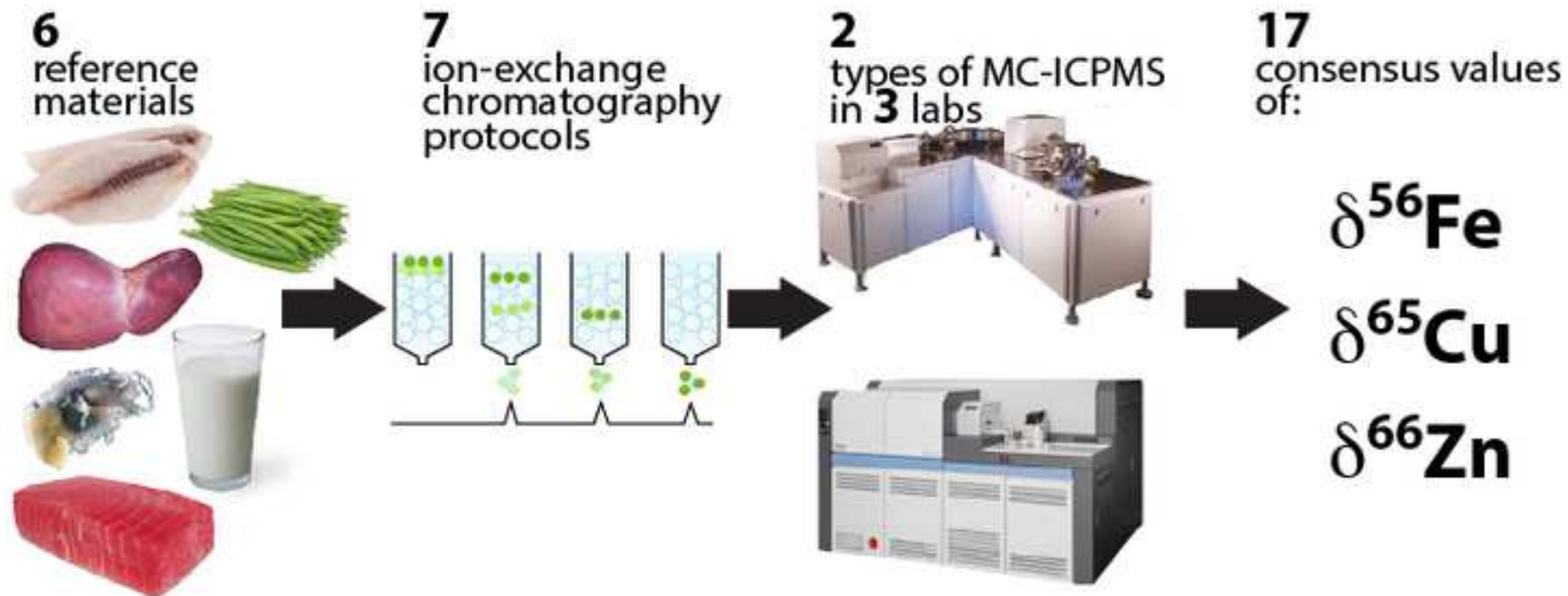
# Talanta

## Inter-comparison of stable iron, copper and zinc isotopic compositions in six reference materials of biological origin --Manuscript Draft--

<b>Manuscript Number:</b>	TAL-D-20-01965R1
<b>Article Type:</b>	Research Paper
<b>Section/Category:</b>	Separation for Bioanalytical applications
<b>Keywords:</b>	reference material, stable isotope, iron, copper, zinc
<b>Corresponding Author:</b>	Vincent Balter Ecole Normale Supérieure de Lyon Lyon, FRANCE
<b>First Author:</b>	Lucie Sauzéat
<b>Order of Authors:</b>	Lucie Sauzéat Marta Costas-Rodríguez Emmanuelle Albalat Nadine Mattielli Frank Vanhaecke Vincent Balter
<b>Abstract:</b>	<p>There is a lack of certified reference materials with an organic matrix for which metal isotope ratios have been certified. Here, we have determined the iron, copper and zinc stable isotopic compositions for six reference materials of biological origin with diverse matrices, i.e. BCR-380R (whole milk), BCR-383 (beans), ERM-CE464 (tuna fish), SRM-1577c (bovine liver), DORM-4 (fish protein) and TORT-3 (lobster hepatopancreas) in three different labs. The concentrations for six major and fifteen trace elements, spanning almost four orders of magnitude, were also measured and the results obtained show an excellent agreement with certified values, demonstrating that the dissolution step was quantitative for all the standards. By taking literature data into account, 39 possible pair-wise comparisons of mean iron, copper and zinc isotopic values (<math>d</math> values) could be made. Results of Tukey multiple comparisons of means yielded 11 significantly pairs. Most of these differences are of the same order of magnitude as the estimated mean expanded uncertainties (<math>U</math>, <math>k = 2</math>) (<math>\pm 0.10</math> ‰, <math>\pm 0.05</math> ‰, and <math>\pm 0.05</math> ‰ for the <math>\delta^{56}\text{Fe}</math>, <math>\delta^{65}\text{Cu}</math> and <math>\delta^{66}\text{Zn}</math> values, respectively). The present inter-comparisons study finally proposes nineteen new isotopic compositions consensus values for six reference materials of biological origin.</p>

Environmental and biological sciences progressively use metal isotope compositions, but metal isotope compositions are sparsely determined in biological reference materials. Here, we offer seventeen consensus values of iron, copper and zinc isotope compositions for six biological reference materials thanks to an inter-laboratory calibration.

Environmental and biological sciences progressively use metal stable isotope ratios  
Metal stable isotope ratios are sparsely determined in biological reference materials  
Consensus value of stable isotope ratios requires inter-laboratory comparisons  
Metal stable isotope ratios consensus values are given for biological reference materials





19 **Abstract**

20 There is a lack of certified reference materials with an organic matrix for which metal isotope ratios  
2  
3  
4  
5  
6  
7  
8  
9  
10  
11  
12  
13  
14  
15  
16  
17  
18  
19  
20  
21  
22  
23  
24  
25  
26  
27  
28  
29  
30  
31  
32  
33  
34  
35  
36  
37  
38  
39  
40  
41  
42  
43  
44  
45  
46  
47  
48  
49  
50  
51  
52  
53  
54  
55  
56  
57  
58  
59  
60  
61  
62  
63  
64  
65

There is a lack of certified reference materials with an organic matrix for which metal isotope ratios have been certified. Here, we have determined the iron, copper and zinc stable isotopic compositions for six reference materials of biological origin with diverse matrices, i.e. BCR-380R (whole milk), BCR-383 (beans), ERM-CE464 (tuna fish), SRM-1577c (bovine liver), DORM-4 (fish protein) and TORT-3 (lobster hepatopancreas) in three different labs. The concentrations for six major and fifteen trace elements, spanning almost four orders of magnitude, were also measured and the results obtained show an excellent agreement with certified values, demonstrating that the dissolution step was quantitative for all the standards. By taking literature data into account, 39 possible pair-wise comparisons of mean iron, copper and zinc isotopic values ( $\delta$  values) could be made. Results of Tukey multiple comparisons of means yielded 11 significantly pairs. Most of these differences are of the same order of magnitude as the estimated mean expanded uncertainties ( $U, k = 2$ ) ( $\pm 0.10 \text{ ‰}$ ,  $\pm 0.05 \text{ ‰}$ , and  $\pm 0.05 \text{ ‰}$  for the  $\delta^{56}\text{Fe}$ ,  $\delta^{65}\text{Cu}$  and  $\delta^{66}\text{Zn}$  values, respectively). The present inter-comparisons study finally proposes nineteen new isotopic compositions preferred values for six reference materials of biological origin.

Keywords: reference material, stable isotope, iron, copper, zinc

## 37 Introduction

38 Involved in a wide range of enzymes and proteins regulating metabolic pathways and  
2  
39 physiological processes [e.g. 1], metals including copper (Cu), iron (Fe) and zinc (Zn), are vital to  
4  
5  
60 the organism and any imbalance can have adverse effects on human health [e.g 2]. In recent times,  
7  
81 in addition to the determination of concentrations, the measurement of stable isotope ratios or  
9  
10  
1142 compositions is evolving into a new tool of choice to study the metabolism of essential mineral  
12  
1343 elements in living organisms, both of plant or animal origin. By definition, isotope fractionation  
14  
15  
1644 refers to changes in the relative abundance of naturally occurring stable isotopes of a particular  
17  
1845 element among coexisting reservoirs hosting this element [e.g. 3]. Vibrational frequencies decrease  
19  
20  
2146 with mass commanding heavy isotopes to be enriched in coordination with the stiffest bonds, in  
22  
2347 particular those involving the oxidized form and with ligands with the stronger electronegativity (O  
24  
2548 > N > S) [3]. So far, the transition metals, iron (Fe), copper (Cu) and zinc (Zn) have been the most  
26  
27  
2849 studied for their isotopic composition in this context.  
29

30  
3150 In plants, the Fe isotopic composition ( $\delta^{56}\text{Fe}$ ) varies according to the type of root uptake and  
32  
3351 shows differences among plant organs [4,5]. In animals, the Fe isotopic compositions are highly  
34  
3552 fractionated between organs [6-8] and provide information on the Fe intestinal absorption efficiency  
36  
37  
3853 [7, 9-11]. In healthy conditions, the blood Fe isotope composition of human males is different from  
39  
4054 that of pre-menopausal females [6] due to menstrual losses [12,13] and the up-regulated Fe  
41  
42  
4355 absorption to compensate for the losses. Varying Fe isotopic composition among blood  
44  
4556 compartments signals different redox processes in red blood cells hemoglobin and in serum  
46  
47  
4857 transferrin [14-17]. For a still unknown reason, the body mass index seems correlated with the  
49  
5058 whole blood Fe isotopic composition [16,17]. The hepatic accumulation of Fe occurs due to  
51  
5259 hereditary hemochromatosis and is reflected in the isotopic composition of Fe in blood [18,19],  
53  
54  
5560 while Fe dysregulations due to various etiologies resulting in anemia [20] can be scrutinized by  
56  
5761 means of the Fe isotopic compositions in whole blood and serum.  
58  
59  
60  
61  
62  
63  
64  
65



62 The Cu isotopes are fractionated during Cu uptake and translocation in plants [21,22]. In  
163 healthy animals, the Cu isotopes are processed slightly differently in the gut via the involvement of  
2  
3  
4  
5  
66 Similarly to Fe, the blood Cu isotopic composition is different between human males and  
7  
8  
9  
10  
11  
12  
13  
14  
15  
16  
17  
18  
19  
20  
21  
22  
23  
24  
25  
26  
27  
28  
29  
30  
31  
32  
33  
34  
35  
36  
37  
38  
39  
40  
41  
42  
43  
44  
45  
46  
47  
48  
49  
50  
51  
52  
53  
54  
55  
56  
57  
58  
59  
60  
61  
62  
63  
64  
65

372 Zinc isotopes in plants are fractionated between all the organs, including roots [22,36]. Zinc  
24  
25  
26  
27  
28  
29  
30  
31  
32  
33  
34  
35  
36  
37  
38  
39  
40  
41  
42  
43  
44  
45  
46  
47  
48  
49  
50  
51  
52  
53  
54  
55  
56  
57  
58  
59  
60  
61  
62  
63  
64  
65

578 Determination of stable isotopic compositions of metals and the corresponding  
58  
59  
60  
61  
62  
63  
64  
65

88 quality control of the results obtained, geological reference materials were thus provided. The  
189 overall quality of the isotope ratio depends not only on the measurement itself, but also profoundly  
2  
3  
4  
5  
6  
7  
8  
9  
10  
11  
12  
13  
14  
15  
16  
17  
18  
19  
20  
21  
22  
23  
24  
25  
26  
27  
28  
29  
30  
31  
32  
33  
34  
35  
36  
37  
38  
39  
40  
41  
42  
43  
44  
45  
46  
47  
48  
49  
50  
51  
52  
53  
54  
55  
56  
57  
58  
59  
60  
61  
62  
63  
64  
65

on the sample preparation. The preparation of the sample involves the dissolution of the sample and the isolation of the metal of interest, typically by ion-exchange chromatography. Geological materials are inorganic and the silicate matrix contains high levels (> 1 %) of metals while the organic matrix of biological materials generally contains metals at trace levels (< 0.1 %). The geological and biological matrices are therefore very different, and the preparation step (dissolution and target element isolation) must be adapted accordingly. As a consequence, geological reference materials cannot be used for the quality control for the processing and analysis of biological samples. To that end, the scientific community devoted to the study of metal isotopic compositions in living systems has reported isotopic values for reference biological materials. A list of the published values is given in **Table S1** for Fe, Cu and Zn isotope compositions. Several observations can be drawn from that compilation. First, the Seronorm reference materials exhibit a significant isotopic heterogeneity between lots for Fe and Cu. Second, the serum matrix seems to be, by itself, highly heterogeneous because the serum reference material BCR-639 has a Cu and Zn isotopic compositions that are substantially different from those of the Seronorm materials. This holds for muscle too, because the two bovine muscle reference materials SRM-8414 and ERM-BB184 have Zn isotopic compositions differing by about ~0.8 ‰. Third, to the best of our knowledge, there is no value published for the Fe and Cu isotopic compositions for reference materials of plant origin.

507 The present study is an effort to fill some of the gaps that exist in the certification of isotopic  
508 compositions of biological reference materials. Here, we have determined the Fe, Cu and Zn stable  
509 isotopic compositions for five biological reference materials with a matrix of animal origin, i.e.  
510 BCR-380R (whole milk), ERM-CE464 (tuna fish), SRM-1577c (bovine liver), NRC-DORM-4 (fish  
511 protein) and NRC-TORT-3 (lobster hepatopancreas), and one biological reference materials with a  
512 matrix of plant origin, BCR-383 (beans). We also have included is an in-house fetal bovine serum  
513 (FBS) as a quality control sample. These isotopic compositions have been measured in three

114 different labs, i.e. the Laboratoire de Géologie de Lyon (hereafter denoted LGL-TPE), Ecole  
115 Normale Supérieure de Lyon, France, the Department of Chemistry, Atomic and Mass  
116 Spectrometry (hereafter denoted A&MS), Ghent University, Belgium and Laboratoire G-TIME  
117 (hereafter denoted G-TIME), Université libre de Bruxelles, Belgium.

118  
119

## 120 **Sample description**

121 The samples consist of six biological reference materials. BCR-380R (whole milk), BCR-  
122 383 (beans) and ERM-CE464 (tuna fish) were purchased from the European Institute for Reference  
123 Materials and Measurements (IRMM), SRM-1577c (bovine liver) was purchased from the US  
124 National Institute of Standard and Technology (NIST), and DORM-4 (fish protein) and TORT-3  
125 (lobster hepatopancreas) from the Canadian National Research Council (NRC). For all these  
126 reference materials, the homogeneity of the initial powder is warranted down to a sample size of  
127 ~100 mg by the institute in which it was prepared. Also included as a quality control sample, is a  
128 fetal bovine serum sample (FBS) sold by Sigma–Aldrich with the lot number 014M3399. The FBS  
129 material was freeze-dried and homogenized in an agate mortar. All materials were stored at the  
130 LGL-TPE. To ensure homogeneity preservation and consistent values between the different  
131 laboratories, all the reference materials were gently shaking before aliquots of at least 1g were  
132 collected and sent to the A&MS and G-TIME labs for analysis.

133  
134

## 135 **Sample digestion**

136 For all sample digestions, and to avoid measurement uncertainties due to heterogeneity of the  
137 reference material powder, a minimum sample size of 100 mg was weighed as recommended by the  
138 three institutes for reference materials.

### 139 LGL-TPE

140 All sample preparation procedures were carried out in clean laminar flow hoods using  
141 double-distilled acids to avoid any exogenous contaminations. Samples were first weighted and

142  
143  
144  
145  
146  
147  
148  
149  
150  
151  
152  
153  
154  
155  
156  
157  
158  
159  
160  
161  
162  
163  
164  
165

140 then dissolved in a mixture of HNO<sub>3</sub> (15 M) and H<sub>2</sub>O<sub>2</sub> (30%) in Savillex® beakers at 120°C for  
141 about 72h. Attention was paid in the first hours because the mixture could be very reactive with the  
142 subsequent formation of nitric and carbon-based fumes that need to be regularly vented to avoid  
143 any overpressure. After complete dissolution, the samples were dried down and subsequently taken  
144 up with 1 mL of HNO<sub>3</sub> (0.5 M) from which a small aliquot was used for the quantitative  
145 determination of major and trace element concentrations.

146

#### 147 A&MS

148

149

150

151

152

153

154

155

156

157

158

159

160

161

162

163

164

165

166

167

168

169

170

171

172

173

174

175

176

177

178

179

180

181

182

183

184

185

186

187

Sample preparation was performed in a class 10 clean lab. The acids used for digestion, HNO<sub>3</sub> (14 M) and HCl (12 M), were purified via sub-boiling distillation. Ultrapure water with a resistivity of  $\geq 18.2 \text{ M}\Omega\cdot\text{cm}$  was obtained from an Element Milli-Q system and used for dilutions. Sample digestion was performed using HNO<sub>3</sub> (14 M) and H<sub>2</sub>O<sub>2</sub> (30%) in closed Teflon Savillex® beakers at 110 °C for 16 h.

#### 188 G-TIME

189

190

191

192

193

194

195

196

197

198

199

200

201

202

203

204

205

206

207

208

209

210

211

212

213

214

Sample preparation was carried out under a class-100 laminar flow hood in a class 1,000 clean room. All the reagents used were purified by sub-boiling distillation and appropriate dilutions were made with 18.2 M $\Omega\cdot\text{cm}$  grade MilliQ water. To mineralize the sample, dry ashing of the sample placed in a pre-cleaned semi-opened ceramic crucible was carried out at 600°C in a muffle furnace for 12h. The powdered samples were transferred into a 15 mL Teflon vial (Savillex®) with 14 M HNO<sub>3</sub> and *suprapur* H<sub>2</sub>O<sub>2</sub> at room temperature, followed by heating on a hot plate for 12-14 h. Samples were then dried down and dissolved using a 1:1 mixture of concentrated HCl and HNO<sub>3</sub>.

## 166 Sample preparation and instrumentation

### 167 LGL-TPE

168 Iron was isolated from the concomitant matrix by ion-exchange chromatography, using a  
169 Bio-Rad column filled with 2 mL of AG 1-X8 (100-200 mesh) anionic resin. After elimination of  
170 the sample matrix with 8 mL of HCl (6 M) with traces of H<sub>2</sub>O<sub>2</sub>, Fe is eluted with 10 mL of HNO<sub>3</sub>  
171 (0.5 M). The procedure was repeated twice to ensure maximum iron purity for optimal isotope  
172 ratio measurements, leading to a total procedure blank of about 10 ng (n = 5), which generally  
173 represents 0.2 to 0.05%, and at worst 1% in the case of BCR380, of the amount of Fe present in the  
174 sample solutions prepared for isotopic analysis. After the purification, Zn remains in the iron  
175 fractions. To evaluate the effect of Zn on the measured iron isotopic compositions of samples, we  
176 added various amounts of an elemental solution of Zn to the IRMM-014 Fe standard solution to  
177 obtain Zn/Fe ratios from 0 to 1. No deviation of the  $\delta^{56}\text{Fe}$  values was observed within the  
178 analytical error (Fig. S1). The elution protocol is given in Table 1.

179 Copper and Zn were isolated by ion-exchange chromatography using a quartz column filled  
180 with 1.8 mL of AG MP-1 (100-200 mesh) anionic resin (Table 1). After elimination of the sample  
181 matrix with 10 mL of HCl (7 M) + H<sub>2</sub>O<sub>2</sub> (0.001%), Cu and Zn were successively eluted with 20  
182 mL of HCl (7 M) + H<sub>2</sub>O<sub>2</sub> (0.001%) and 10 mL of HNO<sub>3</sub> (0.5 M) respectively following the  
183 procedure described by [64]. The procedure was repeated twice leading to total procedural blanks  
184 that were on average 1.4 ng for Cu (n = 6) and 6.7 ng for Zn (n = 6), which represents in average  
185 0.1% and 0.4% of the Cu and Zn amount, respectively, of element present in the sample solutions  
186 prepared for isotopic analysis.

187 The concentrations were measured following the method described in [65] by ICP-OES  
188 (Thermo Scientific, iCap 6000 Radial) for major elements (Na, P, Mg, S, K and Ca) and by ICP-  
189 MS (Thermo Scientific, iCap-Q) for trace elements (Li, V, Cr, Mn, Fe, Co, Ni, Cu, Zn, As, Se, Rb,  
190 Sr, Cd, Ba and Pb). Briefly, the concentrations were calculated using calibration curves based on  
191 multi-elemental solutions. These solutions were also used to monitor and correct for the

192 instrumental drift over the analytical session. Matrix effects and instrumental drift were also  
193 corrected for using In and Sc as internal standards for trace and major elements, respectively.

194 Iron isotopic compositions were measured using a Thermo Scientific Neptune Plus MC-  
195 ICP-MS at LGL-TPE. The instrument settings are given in **Table 2**. On the day of the measurement  
196 session, Fe purified solutions were diluted to 1mg/L and doped with Ni used as an internal  
197 standard to monitor and correct for instrumental mass discrimination. A 1 g/L of Ni elemental  
198 standard solution from Alfa-Aesar was diluted and added to the standard and sample solutions at a  
199 concentration matching the Fe concentration, namely 1 mg/L.

200 The Cu and Zn isotopic compositions were measured by Nu Plasma HR MC-ICP-MS (Nu  
201 Instruments, Nu Plasma HR) following the procedure described by [61], which is synthesized in  
202 **Table 2**. On the day of analyses, Cu and Zn purified solutions were diluted in a Zn-doped solution  
203 (Zn JMC 3-0749L, Johnson Matthey Royston, UK) and a Cu-doped solution (Cu SRM 976,  
204 National Institute of Standards and Technology, Gaithersburg, MD, USA), respectively, to match  
205 the concentration of the standard bracketing solution (usually 300  $\mu\text{g/L}$ ). Measurements were  
206 carried out in static multi-collection mode and one single measurement consisting of 1 block of 30  
207 cycles with an integration time of 10 s.

## 209 A&MS

210 After digestion, the solution was evaporated to dryness and the residue was redissolved in a  
211 mixture of HCl (8 M) and H<sub>2</sub>O<sub>2</sub> (0.001%) and allowed to stand for 1 h to make sure that all of the  
212 iron and copper were in their higher oxidation states. Copper, Fe and Zn were isolated from the  
213 sample matrix using 1 mL of AG-MP1 anion exchange resin, using a revised procedure from  
214 [10,20,31] (**Table 1**). After the sample load and the matrix elution using 3 mL of 8 M HCl +  
215 0.001% H<sub>2</sub>O<sub>2</sub>, Cu, Fe and Zn were sequentially eluted using 9 mL of 5 M HCl+0.001% H<sub>2</sub>O<sub>2</sub>, 7 mL  
216 of 0.6M HCl and 7 mL of 0.7M HNO<sub>3</sub>, respectively. A second chromatographic separation was  
217 applied to the Cu fraction following the same protocol to ensure the complete removal of sodium.

218 The final purified Cu, Fe and Zn fractions were evaporated and re-dissolved in 0.5 mL of 14M  
219 HNO<sub>3</sub> twice to remove residual chlorides. The final residue was re-dissolved in 0.5 mL of 0.28 M  
220 HNO<sub>3</sub>. The overall procedure led to total procedural blanks (n = 4) of about 8 ng for Fe, 0.3 ng for  
221 Cu and 3.0 ng for Zn, which represents less than 1 % of the amount of each element present in the  
222 measurement solutions.

223 A Thermo Scientific Neptune MC-ICP-MS instrument (Germany) was used for all isotope  
224 ratios measurements. Medium mass resolution was used for all isotope ratios to avoid spectral  
225 overlap. Measurements were performed in static collection mode, using Faraday collectors  
226 connected to 10<sup>11</sup> Ω amplifiers. Instrument settings and data acquisition parameters are shown in the  
227 **Table 2**. Fe purified solutions were diluted to 300 µg/L and doped with Ni (300 µg/L) as internal  
228 standard to monitor and correct for instrumental mass discrimination. Cu and Zn solutions were  
229 adjusted to 200 µg/L and doped with Ni and Cu (both at 200 µg/L), respectively. Baseline  
230 correction was performed for each measurement sequence. The in-house elemental standards  
231 A&MS-Cu, A&MS-Fe and A&MS-Zn, previously characterized isotopically [10,20,31], were  
232 included every 5 samples for quality assurance/quality control (QA/QC) of the isotope ratio  
233 measurements.

## 235 G-TIME

236 After complete dissolution, solutions were evaporated to dryness at 125°C and HCl (6 M)  
237 was added to convert the metals into their chloride form prior to the chromatographic separation.  
238 Isolation of Zn was realized using a 2 mL Bio-Rad column loaded with pre-cleaned AG1-X8 100-  
239 200 mesh resin (analytical grade, chloride form) following a modified elution protocol from [64]  
240 (see details in [66]). The sample is re-dissolved in 1mL of 6 M HCl with 20 µl of 30% H<sub>2</sub>O<sub>2</sub> before  
241 loading on the column. The matrix, Cu and Fe were discarded using HCl (8 M) followed by HCl  
242 (0.5 M), and Zn was eluted with 15 mL of 1 M HNO<sub>3</sub> + 0.1 M HBr (**Table 2**). Total procedural  
243 blanks (digestion and chromatography) were less than 10 ng of Zn. Dried Zn fractions were

244 redissolved in 100  $\mu\text{L}$  of concentrated  $\text{HNO}_3$  and then diluted at 400  $\mu\text{g/L}$  in 0.05M  $\text{HNO}_3$  for  
 245 isotope ratio measurements. Cu standard solution was systematically added to samples and  
 246 standards as an internal standard with identical concentrations (400  $\mu\text{g/L}$ ). Zinc isotopes ratios were  
 247 measured on a Nu Plasma II HR MC-ICP-MS (Nu Instruments) with the instrumental settings as  
 248 given in **Table 3**. All Zn and Cu masses ( $^{64}\text{Zn}$ ,  $^{66}\text{Zn}$ ,  $^{67}\text{Zn}$ ,  $^{68}\text{Zn}$ ,  $^{70}\text{Zn}$  and  $^{63}\text{Cu}$ ,  $^{65}\text{Cu}$ ) were monitored,  
 249 as well as  $^{62}\text{Ni}$  to correct for interference between  $^{64}\text{Ni}$  and  $^{64}\text{Zn}$ . However, the  $^{62}\text{Ni}$  beam intensity  
 250 was systematically lower than the background signal ( $\leq 1.10^{-4}$  V). The signals were measured by  
 251 static multi-collection. A single measurement consisted of a measurement of 60 cycles, i.e. 3 blocks  
 252 of 20 cycles (with an integration time of 10 s, each). On-peak baseline measurement with 30 s  
 253 integration time was done prior to each analysis using a 0.05 M  $\text{HNO}_3$  acid blank, and the value  
 254 obtained is then subtracted on-line during the analytical sequence for all the samples/standards.

255  
 256 In all labs and for all isotope ratios measurements, instrumental mass discrimination and  
 257 temporal drift were corrected with an exponential law using an admixed element as internal  
 258 standard, combined with sample- standard bracketing, as recommended by [64]. The doping  
 259 conditions are given in **Table 2**. All the results of isotopic ratios measurements are given in the  
 260 delta annotation (expressed in ‰) and reported relative to the international isotopic standard  
 261 solutions NIST IRMM-014 for Fe, SRM-976 for Cu and JMC 3-0749L for Zn using the following  
 262 equations:

$$\delta^{56}\text{Fe} = \left[ \frac{(^{56}\text{Fe}/^{54}\text{Fe})_{\text{sample}}}{(^{56}\text{Fe}/^{54}\text{Fe})_{\text{standard}}} - 1 \right] \times 1000 \quad [1]$$

$$\delta^{65}\text{Cu} = \left[ \frac{(^{65}\text{Cu}/^{63}\text{Cu})_{\text{sample}}}{(^{65}\text{Cu}/^{63}\text{Cu})_{\text{standard}}} - 1 \right] \times 1000 \quad [2]$$

$$\delta^{66}\text{Zn} = \left[ \frac{(^{66}\text{Zn}/^{64}\text{Zn})_{\text{sample}}}{(^{66}\text{Zn}/^{64}\text{Zn})_{\text{standard}}} - 1 \right] \times 1000 \quad [3]$$

264 All statistical analyses was performed using the R software [67].  
 265



## 265 Results

### 266 Uncertainty estimation for mass fractions

267 The uncertainties given in the present work are expanded uncertainties (denoted  $U$ ),  
268 obtained by multiplying the combined standard uncertainty  $u_c(y)$  of the estimate  $y$  by a coverage  
269 factor  $k$  such that  $U = ku_c(y)$  with  $k = 2$  corresponding to a level of confidence of about 95%.  
270 Following the recommendations of the Guide to the expression of uncertainty in measurement [68],  
271 identified sources of uncertainty ( $x$ ) for the measurement of mass fractions ( $y$ ) relate to instrumental  
272 (variable background stability and counting efficiency) and analytical (error in mass and volume  
273 measurements, contamination). The determination of the combined standard uncertainty can be thus  
274 considered as a linear combination of terms representing the variation of the output estimate  $y$   
275 generated by the uncertainty of each input estimate  $x$  such that:

$$276 \quad u_c^2(y) = \left[ \sum_{i=1}^N c_i u(x_i) \right]^2 \quad [4]$$

277 where  $u_c(y)$  is the combined uncertainty;  $c_i$  the sensitivity coefficient and  $u(x_i)$  the standard  
278 uncertainty which can be estimated by using the standard deviation calculated from replicate  
279 measurements. Here, the sensitivity coefficients were the same for all the measurements and were  
280 not further considered.

281 Excluding contamination as a significant source of uncertainty because the contribution of  
282 the procedural blanks was negligible and all samples were processed in a clean room, other  
283 analytical uncertainties can be considered insignificant compared to instrumental uncertainties  
284 associated with the ICP-MS or ICP-OES techniques, which are at best < 5% (RSD). Comparison of  
285 expanded uncertainties for the determination of major elements ( $n = 18$ ) and trace elements ( $n = 36$ )  
286 are of the same order of magnitude as those determined by NIST, IRMM and NRC (Fig. S2).

## 289 Determination of mass fractions

290 The results of the determination of mass fractions are given in **Table S2**. The number of  
291 measurements ( $n$ ) correspond to the number of aliquots of digested reference materials measured  
292 one time. The table also includes the certified values ( $C_v$ ) when available, allowing to an accuracy  
293 (%) of the measurements ( $M_v$ ) given the relationship:

$$\text{accuracy \%} = 100 - [100 \cdot (C_v M_v) / C_v] \quad [5]$$

294 For all the reference materials and all the elements, the calculation of the accuracy ( $n = 54$ )  
295 showed that the majority of the results have an accuracy  $> 90\%$  (median = 93.0%), with two  
296 outliers, K in DORM-4 (69.5%) and Ni in SRM-1577c (47.8%) resulting in a mean accuracy value  
297 of 91.5% (**Fig. 1**). The overall comparison of the measured values and the certified values showed a  
298 very significant correlation ( $p < 2e^{-16}$  \*\*\*,  $n = 54$ ), spanning more than four orders of magnitude of  
299 mass fraction, a slope close to unity ( $0.993 \pm 0.006$ ) and a small offset of  $0.383 \pm 0.612$  at origin  
300 (**Fig. 2**). The close agreement between measured and certified values whether for trace or major  
301 elements, demonstrates that the digestion step was quantitative at LGL-TPE. By extension to the  
302 other uncertified mass fractions, the present study allows to propose sixty-three new mass fraction  
303 values, i.e. sixteen for BCR-380R, thirteen for BCR-383, three for DORM-4, twenty for ERM-  
304 CE464, one for SRM-1577c and ten for TORT-3 (**Table S2**). These proposed new values are  
305 particularly of interest for the reference materials provided by IRMM (BCR-380R, BCR-383 and  
306 ERM-CE464) which are poorly characterized in terms of elemental mass fractions.

## 308 Uncertainty estimation for isotopic compositions

309 The calculation of the combined standard uncertainty  $u_c(y)$  for an isotope ratio can also be  
310 considered as a linear combination of terms of variations, but the calculation of the combined  
311 standard uncertainty of the delta value involves the uncertainties of the isotope ratios of the sample  
312 and those of the bracketing standard. A full demonstration of the calculation of the combined

313 standard uncertainty of the delta value ( $\delta$ ) is provided by Sullivan et al. [50] and the final equation  
314 is given here for a symbolic  $r^{A/a}$  isotope ratio:

$$u^2(\delta) = \left(\frac{1}{r_{std}^{A/a}}\right)^2 \cdot u^2(r_{spl}^{A/a}) + \left(-\frac{r_{spl}^{A/a}}{r_{std}^{A/a^2}}\right)^2 \cdot u^2(r_{std}^{A/a}) \quad [6]$$

315 where the subscripts *std* and *spl* stand for the standard and the sample, respectively and  $u(r)$  is the  
316 standard uncertainty for measured ratio, which can be estimated by using the standard deviation  
317 calculated from replicate measurements. We have calculated the expanded uncertainties  $U$  for the  
318  $\delta^{56}\text{Fe}$ ,  $\delta^{57}\text{Fe}$ ,  $\delta^{65}\text{Cu}$ ,  $\delta^{66}\text{Zn}$ ,  $\delta^{67}\text{Zn}$  and  $\delta^{68}\text{Zn}$  values which are given in the Table S3 to Table S9 along  
319 with the corresponding isotope ratios. The estimated mean expanded uncertainties were  $\pm 0.10 \text{ ‰}$   
320 for  $\delta^{56}\text{Fe}$  value, and  $\pm 0.05 \text{ ‰}$  for the  $\delta^{65}\text{Cu}$  and  $\delta^{66}\text{Zn}$  values. The magnitude of the expanded  
321 uncertainties for the  $\delta^{65}\text{Cu}$  value is close to that reported by Sullivan et al. [50], i.e.  $\pm 0.07 \text{ ‰}$ . The  
322 higher figure for the  $U$  values associated with the Fe isotopic compositions is due to the fact that  
323 some reference materials (BCR-383, ERM-CE464 and one sample of FBS) at LGL-TPE exhibited  
324 enhanced instability. Reported error values in the present paper are therefore expanded uncertainty  
325  $U$  with a coverage  $k$  factor of two, unless specified otherwise.

### 327 Determination of isotopic compositions

328 All results are given in table Tables S3 to S9. One aspect of the quality of the isotopic  
329 results is assessed by the calculation of the exponent  $\beta$  relating the mass-dependent fractionation  
330 factors for two isotope ratios, which is different for kinetically and thermodynamically controlled  
331 fractionation [69]. Plots of  $\delta^{57}\text{Fe}$  vs  $\delta^{56}\text{Fe}$  (Fig. 3A),  $\delta^{67}\text{Zn}$  vs  $\delta^{66}\text{Zn}$  (Fig. 3B), and  $\delta^{68}\text{Zn}$  vs  $\delta^{66}\text{Zn}$   
332 (Fig. 3C) yield the mass fractionation relationships in three-isotope spaces, allowing to calculate the  
333  $\beta$  values, which correspond to the slopes of the respective linear best-fit regressions. Comparison  
334 with theoretical values (Table 3) show excellent agreement. In biological systems, mass  
335 fractionation is suspected to be under kinetic control, but the calculated  $\beta$  values do not show

336 characteristics of kinetic mass fractionation (Table 3), probably because the fractionation per mass  
337 unit is too small, i.e. < 3‰ estimated by Young et al. [69] using magnesium isotope ratios.

338 Overall, we have considered as valid isotopic data sixty-four measurements of  $\delta^{56}\text{Fe}$  values  
339 (LGL-TPE,  $n = 30$ , A&MS,  $n = 34$ ), eighty-nine measurements of  $\delta^{65}\text{Cu}$  values (LGL-TPE,  $n = 57$ ,  
340 A&MS,  $n = 32$ ) and one hundred measurements of  $\delta^{66}\text{Zn}$  values (LGL-TPE,  $n = 60$ , A&MS,  $n = 34$ ,  
341 G-TIME,  $n = 6$ ).

## 342 Discussion

343 The results of Craddock and Dauphas [53] for the Fe isotopic composition of the SRM-  
344 1577c reference material ( $n = 1$ ) and those of Sullivan et al. [50] for the Cu isotopic compositions  
345 of the DORM-4 ( $n = 6$ ) and TORT-3 ( $n = 6$ ) reference materials can be merged with the present  
346 results ( $n = 253$ ). In order to determine preferred isotopic values, pair-wise comparisons of the  
347 mean isotope ratios have been performed using Tukey's HSD tests. A non-significant associated  $p$   
348 value ( $> 0.05$ ) indicates that the means compared are not different, while an associated  $p$  value ( $<$   
349  $0.05$ ) indicates that the means compared are significantly different. All the results of the possible  
350 pair-wise comparisons are given in the Table S10. Over thirty-nine comparisons, eleven means  
351 were significantly different, ranging from 0.06 ‰ to 0.25 ‰, with an average value of 0.09 ‰  
352 (Table S10). However, most of the differences between the mean values are of the same order of  
353 magnitude as the calculated expanded uncertainties, i.e.  $\pm 0.10$  ‰,  $\pm 0.05$  ‰, and  $\pm 0.05$  ‰ for the  
354  $\delta^{56}\text{Fe}$ ,  $\delta^{65}\text{Cu}$  and  $\delta^{66}\text{Zn}$  values, respectively. Taking the expanded uncertainties into account, only  
355 two differences remain significant, which are between LGL-TPE and A&MS labs for the  $\delta^{65}\text{Cu}$   
356 value of the BCR-380R reference material (0.25 ‰) and between LGL-TPE and G-TIME labs for  
357 the  $\delta^{66}\text{Zn}$  value of the ERM-CE464 reference material (0.14 ‰). These discrepancies might be  
358 explained by incomplete digestion of lipid compounds present in the samples, notably significant  
359 for the BCR-380R and ERM-CE464 reference materials which have a lipid content up to 27 wt%.

361 The final results are shown in Fig. 4, Fig. 5 and Fig. 6 for the  $\delta^{56}\text{Fe}$ ,  $\delta^{65}\text{Cu}$  and  $\delta^{66}\text{Zn}$   
362 values, respectively. The  $\delta^{56}\text{Fe}$  values range from -1.92 ‰ to  $\sim$  -0.22 ‰, representing a span of  
363 variation of 0.65 ‰ per mass unit (Fig. 4). The range of variation is 0.75 ‰ per mass unit for the  
364  $\delta^{65}\text{Cu}$  values (min. = -0.15 ‰, max. = 1.32 ‰, Fig. 5) and 0.70 ‰ per mass unit for the  $\delta^{66}\text{Zn}$   
365 values (min. = -0.44 ‰, max. = 0.97 ‰, Fig. 6).

366 The  $\delta^{56}\text{Fe}$  values for the SRM-1577c reference material reported by Craddock and Dauphas  
367 [53] is  $-1.34 \pm 0.03$  ‰ ( $\pm 2\text{SD}$ ), in accordance with the values determined at LGL-TPE ( $-1.36$   
368  $\pm 0.06$  ‰) and A&MS ( $-1.29 \pm 0.08$  ‰) (Table S8). The present Fe isotopic composition completes  
369 well the reduced variability already measured on whole blood reference materials, which  
370 permanently exhibit very low  $\delta^{56}\text{Fe}$  values  $< -2$  ‰ (Table S1). The DORM-4 reference material  
371 displays the highest  $\delta^{56}\text{Fe}$  value determined here ( $-0.26 \pm 0.07$  ‰, Fig. 4). DORM-4 is a fish protein  
372 homogenate but it is not specified whether it was prepared from a freshwater or a seawater fish. The  
373 Fe isotopic compositions of the tuna fish muscle ERM-CE464 reference material ( $-0.60 \pm 0.09$  ‰,  
374 Fig. 4) and the already measured shrimp and tuna muscles [6] exhibit slightly negative values,  
375 suggesting that the DORM-4 reference material was likely prepared from seawater fish. Note that  
376 the TORT-3 reference material, which is also produced from a seawater animal (lobster), has a  
377 negative  $\delta^{56}\text{Fe}$  value ( $-1.41 \pm 0.10$  ‰), showing that the Fe isotope fractionation between organs is  
378 probably important in the entire animal kingdom. Regarding plants, the bean BCR-383 reference  
379 material also has a slightly negative  $\delta^{56}\text{Fe}$  value ( $-0.33 \pm 0.09$  ‰, Fig. 4), in accordance with the  
380 values found by Walczyk and von Blanckenburg [6].

381 The  $\delta^{65}\text{Cu}$  values for the DORM-4 reference material reported by Sullivan et al. [50] is  $0.52$   
382  $\pm 0.06$  ‰, in accordance with the values determined at LGL-TPE ( $0.47 \pm 0.04$  ‰) and A&MS ( $0.45$   
383  $\pm 0.04$  ‰) (Table S5). This also holds for the  $\delta^{65}\text{Cu}$  value of the TORT-3 reference material which  
384 was measured at  $0.35 \pm 0.04$  ‰ at LGL-TPE,  $0.34 \pm 0.04$  ‰ at A&MS, and  $0.36 \pm 0.05$  ‰ at  
385 DGSGE (Table S9). The  $\delta^{65}\text{Cu}$  values obtained in the present study are within the range of those

386 already reported for this reference material (Table S1). The FBS serum material, used as a quality  
387 control sample and not a reference material, shows a high  $\delta^{65}\text{Cu}$  value ( $1.22 \pm 0.07 \text{‰}$ , Fig. 5). The  
388 fish protein DORM4 reference material has a  $\delta^{65}\text{Cu}$  value of  $0.48 \pm 0.06 \text{‰}$ , different from that of  
389 the dogfish liver DOLT-5 ( $-0.02 \pm 0.08 \text{‰}$ ,  $\pm 2\text{SD}$ ) (Table S1), which demonstrates that isotope  
390 fractionation among organs of lower vertebrates also takes place for Cu. Regarding plant, the  $\delta^{65}\text{Cu}$   
391 value of the bean BCR-383 reference material is close to 0 ‰ ( $-0.05 \pm 0.05 \text{‰}$ , Fig. 5).

392 The  $\delta^{66}\text{Zn}$  values determined in the present study range within the variability of the values  
393 already published for reference materials, i.e. between  $-0.4 \text{‰}$  and  $1.1 \text{‰}$  (Table S1). BCR-639  
394 exhibits a very negative value ( $\sim -3 \text{‰}$ , [41; 51], Table S1), which is unusual regarding the known  
395 Zn isotopic variability. The BCR-639 reference material is a “high-level” serum that has been  
396 doped with trace elements, and we think that it contains added Zn, probably highly purified Zn,  
397 with a negative  $\delta^{66}\text{Zn}$  value (Rehkämper M., Pers. Comm.). As for Cu, the FBS serum material has  
398 a high  $\delta^{66}\text{Zn}$  value ( $0.92 \pm 0.05 \text{‰}$ , Fig. 6). The other biological reference materials of animal origin  
399 show  $\delta^{66}\text{Zn}$  values ranging from  $\sim -0.3 \text{‰}$  for the tuna fish muscle ERM-CE464 to  $\sim +0.5 \text{‰}$  for the  
400 whole milk BCR-380R, probably produced from cow milk (Fig. 6).

401 The results presented in this paper may be helpful for those researchers exploring high-  
402 precision isotopic analysis of Cu, Fe and/or Zn in biological and clinical sciences, providing them  
403 with a precious and sensitive tool for the quality control of their results.

#### 405 **Acknowledgements**

406 V.B. and L.S. are grateful to Fondation Bullukian, Fondation Mérieux, the CNRS Mission pour  
407 l’Interdisciplinarité as well as the Ecole Polytechnique Fédérale of Lausanne (P. Gillet) for their  
408 financial support. Lu Yang is thanked for sharing the raw Cu isotopic data of the DORM-4 and  
409 TORT-3 reference materials. M.C.-R. acknowledges the Flemish Research Foundation (FWO) for  
410 her postdoctoral grant. F.V. acknowledges FWO for providing the funding for the acquisition of  
411 MC-ICP-MS instrumentation (ZW15-02 – G0H6216N). NM thanks Jeroen de Jong and Wendy

412 Debouge for their assistance during the analytical work. NM acknowledges the F.R.S-FNRS for its  
413 precious financial support in the G-Time instrumental platform development.

2  
3  
414

5  
415 **References**

7  
8  
416 [1] K.J. Waldron and N.J. Robinson. How do bacterial cells ensure that metalloproteins get the  
9 correct metal? *Nat. Rev. Microbiol.* 7 (2009) 25-35.

10  
11  
418 [2] K.J. Barnham and A.I. Bush. Biological metals and metal-targeting compounds in major  
12 neurodegenerative diseases. *Chem. Soc. Rev.* 43 (2014) 6727-6749.

13  
14  
421 [3] F. Albarède, P. Télouk, V. Balter. Medical applications of isotope metallomics. *Measurements,*  
15 *Theories and Applications of non-Traditional Stable Isotopes.* *Rev. Mineral. Geochem.* 82 (2017)  
16 851-885.

17  
18  
425 [4] M. Guelke and F. von Blanckenburg, Fractionation of stable iron isotopes in higher plants.  
19 *Environ. Sci. Technol.* 41 (2007) 1896-1901.

20  
21  
426 [5] M. Kiczka, J.G. Wiederhold, S.M. Kraemer, B. Bourdon and R. Kretzschmar, Iron Isotope  
22 Fractionation during Fe Uptake and Translocation in Alpine Plants. *Environ. Sci. Technol.* 44  
23 (2010) 6144-6150.

24  
25  
429 [6] T. Walczyk and F. von Blanckenburg, Natural iron isotope variations in human blood. *Science*  
26 295 (2002) 2065-2067.

27  
28  
432 [7] K. Hotz, H. Augsburg and T. Walczyk, Isotopic signatures of iron in body tissues as a  
29 potential biomarker for iron metabolism. *J. Anal. At. Spectrom.* 26 (2011) 1347-1353.

30  
31  
435 [8] V. Balter, A. Lamboux, A. Zazzo, P. Télouk, Y. Leverrier, J. Marvel, A.P. Moloney, F.J.  
32 Monahan, O., Schmidt and F. Albarède, Contrasting Fe, Cu, and Zn isotopic patterns in organs and  
33 body fluids of mice and sheep, with emphasis on cellular fractionation. *Metallomics* 5 (2013) 1470-  
34 1482.

35  
36  
438 [9] K. Hotz and T. Walczyk, Natural iron isotopic composition of blood is an indicator of dietary  
37 iron absorption efficiency in humans. *J. Biol. Inorg. Chem.* 18 (2013) 1-7.

38  
39  
441 [10] L. Van Heghe, E. Engström, I. Rodushkin, C. Cloquet and F. Vanhaecke, Isotopic analysis of  
40 the metabolically relevant transition metals Cu, Fe and Zn in human blood from vegetarians and  
41 omnivores using multi-collector ICP-mass spectrometry. *J. Anal. At. Spectrom.* 27 (2012) 1327-  
42 1334.

43  
44  
444 [11] M.R. Flórez, Y. Anoshkina, M. Costas-Rodríguez, C. Grootaert, J. Van Camp, J. Delanghe and  
45 F. Vanhaecke, Natural Fe isotope fractionation in an intestinal Caco-2 cell line model. *J. Anal. At.*  
46 *Spectrom.* 32 (2017) 1713-1720.

47  
48  
449 [12] L. Van Heghe, O. Deltombe, J. Delanghe, H. Depypere and F. Vanhaecke, The influence of  
49 menstrual blood loss and age on the isotopic composition of Cu, Fe and Zn in human whole blood.  
50 *J. Anal. At. Spectrom.* 29 (2014) 478-482.

51  
52  
53  
54  
55  
56  
57  
58  
59  
60  
61  
62  
63  
64  
65

- 460 [13] K. Jaouen and V. Balter, Menopause effect on blood Fe and Cu isotope compositions. *Am. J.*  
461 *Phys. Anthropol.* 153 (2014) 280-285.
- 462  
463 [14] F. Albarède, P. Télouk, A. Lamboux, K. Jaouen and V. Balter, Isotopic evidence of  
464 unaccounted for Fe and Cu erythropoietic pathways. *Metallomics* 3 (2011) 926-933.
- 465  
466 [15] F. von Blanckenburg, M. Oelze, D.G. Schmid, K. van Zuilen, H.P. Gschwind, A.J. Slade, S.  
467 Stitah, D. Kaufmann and P. Swart, An iron stable isotope comparison between human erythrocytes  
468 and plasma. *Metallomics* 6 (2014) 2052-2061.
- 469  
470 [16] Y.-H. Liang, K.-Y.A. Huang, D.-C. Lee, K.-N. Pang and S.-H. Chen, High-precision iron  
471 isotope analysis of whole blood, erythrocytes, and serum in adults. *J. Trace Elem. Med. Biol.* 58  
472 (2020) 126421.
- 473  
474 [17] J.C. Cikomola, M.R. Flórez, M. Costas-Rodríguez, Y. Anoshkina, K. Vandepoele, P.B.  
475 Katchunga, A.S. Kishabongo, M.M. Speeckaert, F. Vanhaecke and J.R. Delanghe, Whole blood Fe  
476 isotopic signature in a sub-Saharan African population. *Metallomics* 9 (2017) 1142-1149.
- 477  
478 [18] P.-A. Krayenbuehl, T. Walczyk, R. Schoenberg, F. von Blanckenburg and G. Schulthess,  
479 Hereditary hemochromatosis is reflected in the iron isotope composition of blood. *Blood* 105  
480 (2005) 3812-3816.
- 481  
482 [19] A. Stenberg, D. Malinovsky, B. Öhlander, H. Andrén, W. Forsling, L.-M. Engström, A.  
483 Wahlin, E. Engström, I. Rodushkin and D.C. Baxter, Measurement of iron and zinc isotopes in  
484 human whole blood: Preliminary application to the study of HFE genotypes. *J. Trace Elem. Med.*  
485 *Biol.* 19 (2005) 55-60.
- 486  
487 [20] Y. Anoshkina, M. Costas-Rodríguez, M. Speeckaert, W. Van Biesen, J. Delanghe and F.  
488 Vanhaecke, Iron isotopic composition of blood serum in anemia of chronic kidney disease.  
489 *Metallomics* 9 (2017) 517-524.
- 490  
491 [21] C. Weinstein, F. Moynier, K. Wang, R. Paniello, J. Foriel, J. Catalano and S. Pichat, Isotopic  
492 fractionation of Cu in plants. *Chem. Geol.* 286 (2011) 266-271.
- 493  
494 [22] D. Jouvin, D.J. Weiss, T.F.M. Mason, M.N. Bravin, P. Louvat, F. Zhao, F. Ferec, P. Hinsinger  
495 and M.F. Benedetti, Stable isotopes of Cu and Zn in higher plants: evidence for Cu reduction at the  
496 root surface and two conceptual models for isotopic fractionation processes. *Environ. Sci. Technol.*  
497 46 (2012) 2652–2660.
- 498  
499 [23] K.A. Miller, F.A. Vicentini, S.A. Hirota, K.A. Sharkey and M.E. Wieser, Antibiotic treatment  
500 affects the expression levels of copper transporters and the isotopic composition of copper in the  
501 colon of mice. *Proc. Natl Acad. Sci. USA*, 116 (2019) 5955–5960.
- 502  
503 [24] M. Costas-Rodríguez, S. Van Campenhout, A.A.M.B. Hastuti, L. Devisscher, H. Van  
504 Vlierberghe and F. Vanhaecke, Body distribution of stable copper isotopes during the progression  
505 of cholestatic liver disease induced by common bile duct ligation in mice. *Metallomics* 11 (2019)  
506 1093-1103.
- 507  
508 [25] K. Jaouen, M. Gibert, A. Lamboux, P. Télouk, F. Fourel, F. Albarède, A.N. Alekseev, E.  
509 Crubézy, and V. Balter, Is aging recorded in blood Cu and Zn isotope compositions? *Metallomics* 5  
510 (2013) 1016-1024.

611  
62  
63  
64  
65



- 512 [26] L. Sauzéat, A. Laurençon and V. Balter, Metallome evolution in ageing *C. elegans* and a  
513 copper stable isotope perspective. *Metallomics* 10 (2018) 496-503.
- 514  
515 [27] M. Aramendía, L. Rello, M. Resano and F. Vanhaecke, Isotopic analysis of Cu in serum  
516 samples for diagnosis of Wilson's disease: a pilot study. *J. Anal. At. Spectrom.* 28 (2013) 675-681.
- 517  
518 [28] M. Resano, M. Aramendía, L. Rello, M.L. Calvo, S. Bérail and C. Pécheyran, Direct  
519 determination of Cu isotope ratios in dried urine spots by means of fs-LA-MC-ICPMS. Potential to  
520 diagnose Wilson's disease. *J. Anal. At. Spectrom.* 28 (2013) 98-106.
- 521  
522 [29] V. Balter, A. Nogueira da Costa, V.P. Bondanese, K. Jaouen, A. Lamboux, S. Sangrajrang, N.  
523 Vincent, F. Fourel, P. Télouk, M. Gigou, C. Lécuyer, P. Srivatanakul, C. Bréchet, F. Albarède and  
524 P. Hainaut, Natural variations of copper and sulfur stable isotopes in blood of hepatocellular  
525 carcinoma patients. *Proc. Natl Acad. Sci. USA* 112 (2015) 982-985.
- 526  
527 [30] L. Lobo, M. Costas-Rodríguez, J.C. de Vicente, R. Pereiro, F. Vanhaecke and A. Sanz-Medel,  
528 Elemental and isotopic analysis of oral squamous cell carcinoma tissues using sector-field and  
529 multi-collector ICP-mass spectrometry. *Talanta* 165 (2017) 92-97.
- 530  
531 [31] M. Costas-Rodríguez, Y. Anoshkina, S. Lauwens, H. Van Vlierberghe, J. Delanghe and F.  
532 Vanhaecke, Isotopic analysis of Cu in blood serum by multi-collector ICP-mass spectrometry: a  
533 new approach for the diagnosis and prognosis of liver cirrhosis? *Metallomics* 7 (2015) 491-498.
- 534  
535 [32] K.A. Miller, C.M. Keenan, G.R. Martin, F.R. Jirik, K.A. Sharkey and M.E. Wieser, The  
536 expression levels of cellular prion protein affect copper isotopic shifts in the organs of mice. *J.*  
537 *Anal. At. Spectrom.* 31 (2016) 2015-2022.
- 538  
539 [33] T.G. Enge, H. Ecroyd, D.F. Jolley, J.J. Yerbury and A. Dosseto, Longitudinal assessment of  
540 metal concentrations and copper isotope ratios in the G93A SOD1 mouse model of amyotrophic  
541 lateral sclerosis. *Metallomics* 9 (2017) 161-174.
- 542  
543 [34] F. Moynier, J. Creech, J. Dallas and M. Le Borgne, Serum and Brain natural copper stable  
544 isotopes in a mouse model of Alzheimer's disease. *Sci. Rep.* 9 (2019) 1-7.
- 545  
546 [35] L. Sauzéat, E. Bernard, A. Perret-Liaudet, I. Quadrio, A. Vighetto, P. Krolak-Salmon, E.  
547 Broussolle, P. Leblanc and V. Balter, Isotopic evidence for disrupted copper metabolism in  
548 amyotrophic lateral sclerosis. *iScience* 6 (2018) 264-271.
- 549  
550 [36] F. Moynier, S. Pichat, M.L. Pons, V. Balter, D. Fike and F. Albarède, Isotopic fractionation  
551 and transport mechanisms of Zn in plants. *Chem. Geol.* 267 (2009) 125-130.
- 552  
553 [37] V. Balter, A. Zazzo, A. Moloney, F. Moynier, O. Schmidt, F. Monahan and F. Albarède,  
554 Bodily variability of zinc natural isotope abundances in sheep. *Rapid Comm. Mass Spectrom.* 24  
555 (2010) 605-612.
- 556  
557 [38] B. Mahan, F. Moynier, A.L. Jørgensen, M. Habekost and J. Siebert, Examining the  
558 homeostatic distribution of metals and Zn isotopes in Göttingen minipigs. *Metallomics* 10 (2018)  
559 1264-1281.
- 560  
561 [39] R.E.T. Moore, M. Rehkämper, W. Maret and F. Larner, Assessment of coupled Zn  
562 concentration and natural stable isotope analyses of urine as a novel probe of Zn status.  
563 *Metallomics* 11 (2019) 1506-1517.

- 564  
565 [40] F. Moynier, J. Foriel, A.S. Shaw and M. Le Borgne, Distribution of Zn isotopes during  
566 Alzheimer's disease. *Geochem. Perspect. Lett.* 3 (2017) 142-150.
- 567  
568 [41] F. Larner, L.N. Woodley, S. Shousha, A. Moyes, E. Humphreys-Williams, S. Strekopytov,  
569 A.N. Halliday, M. Rehkämper and R.C. Coombes, Zinc isotopic compositions of breast cancer  
570 tissue. *Metallomics* 7 (2015) 107-112.
- 571  
572 [42] K. Schilling, F. Larner, A. Saad, R. Roberts, H.M. Kocher, O. Blyuss, A.N. Halliday and T.  
573 Crnogorac-Jurcevic, Urine metallomics signature as an indicator of pancreatic cancer. *Metallomics*  
574 (2020)
- 575  
576 [43] A. Büchl, C.J. Hawkesworth, K.V. Ragnarsdottir and D.R. Brown, Re-partitioning of Cu and  
577 Zn isotopes by modified protein expression. *Geochem. Trans.* 9 (2008) 11.
- 578  
579 [44] S.C. Yang, L. Welter, A. Kolatkar, J. Nieva, K.R. Waitman, K.F. Huang, W.H. Liao, S.  
580 Takano, W.M. Berelson, A.J. West, P. Kuhn and S.G. John, A new anion exchange purification  
581 method for Cu stable isotopes in blood samples. *Anal. Bioanal. Chem.* 411 (2019) 765-776.
- 582  
583 [45] A. Stenberg, I. Malinovsky, I. Rodushkin, H. Andrén, C. Pontér, B. Öhlander and D.C. Baxter,  
584 Separation of Fe from whole blood matrix for precise isotopic ratio measurements by MC-ICP-MS:  
585 a comparison of different approaches. *J. Anal. At. Spectrom.* 18 (2003) 23–28.
- 586  
587 [46] A. Stenberg, I. H. Andrén, I. Malinovsky, E. Engström, I. Rodushkin, and D.C. Baxter,  
588 Isotopic variations of Zn in biological materials. *Anal. Chem.* 76 (2004) 3971-3978.
- 589  
590 [47] S. Lauwens, M. Costas-Rodríguez and F. Vanhaecke, Ultra-trace Cu isotope ratio  
591 measurements via multi-collector ICP mass spectrometry using Ga as internal standard: an  
592 approach applicable to micro-samples. *Anal. Chim. Acta*, 1025 (2018) 69-79.
- 593  
594 [48] S. Lauwens, M. Costas-Rodríguez, H. Van Vlierberghe, and F. Vanhaecke, Cu isotopic  
595 signature in blood serum of liver transplant patients: a follow-up study. *Sci. Rep.* 6 (2016) 30683.
- 596  
597 [49] S. Lauwens, M. Costas-Rodríguez, H. Van Vlierberghe, and F. Vanhaecke, High-precision  
598 isotopic analysis of Cu in blood serum via multi-collector ICP-mass spectrometry for clinical  
599 investigation: steps towards improved robustness and higher sample throughput. *J. Anal. At.*  
600 *Spectrom.* 32 (2017) 597-608.
- 601  
602 [50] K. Sullivan, D. Layton-Matthews, M. Leybourne, J. Kidder, Z. Mester and L. Yang, Copper  
603 isotopic analysis in geological and biological reference materials by MC-ICP-MS. *Geostand.*  
604 *Geoanal. Res.* (2020).
- 605  
606 [51] R.E.T. Moore, F. Larner, B.J. Coles and M. Rehkämper, High precision zinc stable isotope  
607 measurement of certified biological reference materials using the double spike technique and  
608 multiple collector-ICP-MS. *Anal. Bioanal. Chem.* 409 (2017) 2941–2950.
- 609  
610 [52] M. Costas-Rodríguez, L. Van Heghe and F. Vanhaecke, Evidence for a possible dietary effect  
611 on the isotopic composition of Zn in blood via isotopic analysis of food products by multi-collector  
612 ICP-mass spectrometry. *Metallomics* 6 (2014) 139-146.
- 613  
614 [53] P.R. Craddock and N. Dauphas, Iron isotopic compositions of geological reference materials  
615 and chondrites. *Geostand. Geoanal. Res.* 35 (2011) 101-123.
- 62  
63  
64  
65

- 616  
617 [54] C.N. Maréchal, E. Nicolas, C. Douchet and F. Albarède, Abundance of zinc isotopes as a  
618 marine biogeochemical tracer. *Geochem. Geophys. Geosyst.* 1 (2000) 10.1019/1999GC000029  
619  
620 [55] T. Arnold, M. Schönbacher, M. Rehkämper, S. Dong, F.-J. Zhao, G.J.D. Kirk, B.J. Coles and  
621 D.J. Weiss, Measurement of zinc stable isotope ratios in biogeochemical matrices by double-spike  
622 MC-ICPMS and determination of the isotope ratio pool available for plants from soil. *Anal.*  
623 *Bioanal. Chem.* 398 (2010) 3115–3125.  
624  
625 [56] D.J. Weiss, N. Rausch, T.F.D. Mason, B.J. Coles, J.J. Wilkinson, L. Ukonmaanaho, T. Arnold  
626 and T.M. Nieminen, Atmospheric deposition and isotope biogeochemistry of zinc in ombrotrophic  
627 peat. *Geochim. Cosmochim. Acta* 71 (2007) 3498–3517.  
628  
629 [57] E. Smolders, L. Versieren, D. Shuofei, N. Mattielli, D. Weiss, I. Petrov and F. Degryse,  
630 Isotopic fractionation of Zn in tomato plants suggests the role of root exudates on Zn uptake. *Plant*  
631 *Soil* 370 (2013) 605–613.  
632  
633 [58] C. Caldelas, S. Dong, J.L. Araus and D.J. Weiss, Zinc isotopic fractionation in *Phragmites*  
634 *australis* in response to toxic levels of zinc. *J. Experiment. Bot.* 62 (2011) 2169–2178.  
635  
636 [59] J. Viers, P. Oliva, A. Nonell, A. Gélabert, J.E. Sonke, R. Freydier, R. Gainville and B. Dupré,  
637 Evidence of Zn isotopic fractionation in a soil–plant system of a pristine tropical watershed (Nsimi,  
638 Cameroon). *Chem. Geol.* 239 (2007) 124–137.  
639  
640 [60] C. Cloquet, J. Carignan and G. Libourel, Isotopic composition of Zn and Pb atmospheric  
641 depositions in an urban/periurban area of Northeastern France. *Environ. Sci. Technol.* 40 (2006)  
642 6594–6600.  
643  
644 [61] L. Dinis, P. Gammon, M.M. Savard, C. Bégin, I. Girard and J. Vaive, Puzzling Zn isotopes in  
645 spruce tree-ring series. *Chem. Geol.* 476 (2018) 171–179.  
646  
647 [62] J.E. Sonke, Y. Sivry, J. Viers, R. Freydier, L. Dejong, L. André, J.K. Aggarwal, F. Fontan and  
648 B. Dupré, Historical variations in the isotopic composition of atmospheric zinc deposition from a  
649 zinc smelter. *Chem. Geol.* 252 (2008) 145–157.  
650  
651 [63] Y.-T. Tang, C. Cloquet, T. Sterckeman, G. Echevarria, J. Carignan, R.-L. Qiu and J.-L. Morel,  
652 Fractionation of stable zinc isotopes in the field-grown zinc hyperaccumulator *Noccaea*  
653 *caerulescens* and the zinc-tolerant plant *silene vulgaris*. *Environ. Sci. Technol.* 46 (2012) 9972–  
654 9979.  
655  
656 [64] C.N. Maréchal, P. Télouk and F. Albarède, Precise analysis of copper and zinc isotopic  
657 compositions by plasma-source mass spectrometry. *Chem. Geol.* 156 (1999) 251–273.  
658  
659 [65] M. Garçon, L. Sauzéat, R.W. Carlson, S.B. Shirey, M. Horan, M. Simon, V. Balter and M.  
660 Boyet, Nitrile, latex, neoprene and vinyl gloves: a primary source of contamination for trace  
661 element and Zn isotopic analyses in geological and biological samples. *Geostand Geoanal. Res.* 41  
662 (2017) 367–380.  
663  
664 [66] A. Vanderstraeten, S. Bonneville, S. Gili, J. de Jong, W. Debouge, P. Claeys and N. Mattielli,  
665 First multi-isotopic (Pb-Nd-Sr-Zn-Cu-Fe) characterisation of dust reference materials (ATD and  
666 BCR-723): a multi-column chromatographic method optimised to trace mineral and anthropogenic  
667 dust sources. *Geostand. Geoanal. Res.*

- 668  
669 [67] R Core Team, R: A language and environment for statistical computing. R Foundation for  
670 Statistical Computing, Vienna, Austria. (2013) URL <http://www.R-project.org/>.  
671  
672 [68] JCGM 100, Evaluation of measurement data – Guide to the expression of uncertainty in  
673 measurement (ISO/IEC Guide 98-3).  
674  
675 [69] E.D. Young, A. Galy and H. Nagahara, Kinetic and equilibrium mass-dependent isotope  
676 fractionation laws in nature and their geochemical and cosmochemical significance. *Geochim.*  
677 *Cosmochim. Acta* 66 (2002) 1095-1104.  
678  
679

13  
14  
15 **Figure captions**

16  
17 Figure 1

18  
19  
20 Distribution of mass fraction values accuracy (%) in reference materials from this study. The  
21  
22 summary of the distribution parameters is indicated. The grey shaded area corresponds to the  
23  
24 density of the distribution of the accuracy of the results.  
25

26  
27  
28  
29 Figure 2

30  
31  
32 Correlation between certified and measured mass fraction values ( $\mu\text{g/g}$ ) in the reference materials  
33  
34 analyzed in this study. The linear regression parameters are indicated along with the correlation  
35  
36 coefficient and the associated  $p$  value. Error bars are  $U$  ( $k = 2$ ).  
37  
38

39  
40  
41 Figure 3

42  
43  
44 Mass fractionation in three-isotope space for the reference materials analyzed in this study; A)  $\delta^{57}\text{Fe}$   
45  
46 vs  $\delta^{56}\text{Fe}$ ; B)  $\delta^{67}\text{Zn}$  vs  $\delta^{66}\text{Zn}$ ; C)  $\delta^{68}\text{Zn}$  vs  $\delta^{66}\text{Zn}$ . In all cases, the correlation coefficient and the  
47  
48 associated  $p$  value are indicated. The linear regression parameters are given in Table 3. Error bars  
49  
50 are  $U$  ( $k = 2$ ).  
51  
52

53  
54  
55  
56 Figure 4

57  
58  
59 Distribution of the  $\delta^{56}\text{Fe}$  values in reference materials analyzed in this study. Preferred  $\delta^{56}\text{Fe}$  values  
60  
61  
62  
63  
64  
65

699 are indicated. Error associated to the preferred value is the mean of  $U$  ( $k = 2$ ) of each aliquot  
700 digested and processed according to the chromatographic procedure. The  $n^*$  value corresponds to  
701 the number of these aliquots. Error bars are  $U$  ( $k = 2$ ). Origins stands for the lab of Craddock and  
702 Dauphas [53].

704 Figure 5

705 Distribution of the  $\delta^{65}\text{Cu}$  values in reference materials analyzed in this study. Preferred  $\delta^{65}\text{Cu}$  values  
706 are indicated. Error associated to the preferred value is the mean of  $U$  ( $k = 2$ ) of each aliquot  
707 digested and processed according to the chromatographic procedure. The  $n^*$  value corresponds to  
708 the number of these aliquots. Error bars are  $U$  ( $k = 2$ ). DGSGE stands for the lab (Department of  
709 Geological Sciences and Geological Engineering) of Sullivan et al. [50].

711 Figure 6

712 Distribution of the  $\delta^{66}\text{Zn}$  values in reference materials analyzed in this study. Preferred  $\delta^{65}\text{Cu}$  values  
713 are indicated. Error associated to the preferred value is the mean of  $U$  ( $k = 2$ ) of each aliquot  
714 digested and processed according to the chromatographic procedure. The  $n^*$  value corresponds to  
715 the number of these aliquots. Error bars are  $U$  ( $k = 2$ ).

717 **Table captions**

718 Table 1

719 Ion exchange protocols for the chromatographic separation of Cu, Fe and Zn.

721 Table 2

722 Instrument settings and data acquisition parameters for MC-ICP-MS analysis.

726 Linear regression parameters for the observed mass fractionations. The theoretical slope ( $\beta$ ) values  
2  
3  
727 are given for kinetically and thermodynamically controlled mass fractionations for comparison.

5  
6  
7  
8  
9  
10  
11  
12  
13  
14  
15  
16  
17  
18  
19  
20  
21  
22  
23  
24  
25  
26  
27  
28  
29  
30  
31  
32  
33  
34  
35  
36  
37  
38  
39  
40  
41  
42  
43  
44  
45  
46  
47  
48  
49  
50  
51  
52  
53  
54  
55  
56  
57  
58  
59  
60  
61  
62  
63  
64  
65

1  
2  
3  
4  
5  
6  
7  
8  
9  
10  
11  
12  
13  
14  
15  
16  
17  
18  
19  
20  
21  
22  
23  
24  
25  
26  
27  
28  
29  
30  
31  
32  
33  
34  
35  
36  
37  
38  
39  
40  
41  
42  
43  
44  
45  
46  
47  
48  
49  
50  
51  
52  
53  
54  
55  
56  
57  
58  
59  
60  
61  
62  
63  
64  
65

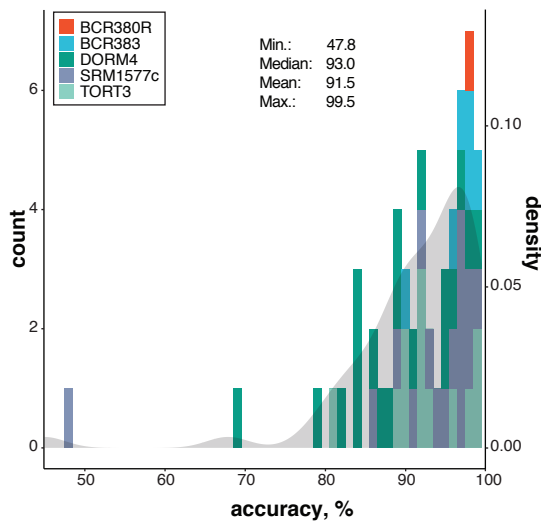


FIGURE 1

1  
2  
3  
4  
5  
6  
7  
8  
9  
10  
11  
12  
13  
14  
15  
16  
17  
18  
19  
20  
21  
22  
23  
24  
25  
26  
27  
28  
29  
30  
31  
32  
33  
34  
35  
36  
37  
38  
39  
40  
41  
42  
43  
44  
45  
46  
47  
48  
49  
50  
51  
52  
53  
54  
55  
56  
57  
58  
59  
60  
61  
62  
63  
64  
65

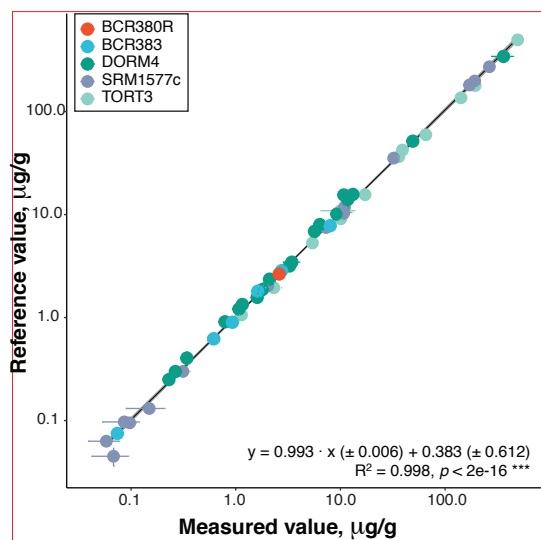


FIGURE 2



1  
2  
3  
4  
5  
6  
7  
8  
9  
10  
11  
12  
13  
14  
15  
16  
17  
18  
19  
20  
21  
22  
23  
24  
25  
26  
27  
28  
29  
30  
31  
32  
33  
34  
35  
36  
37  
38  
39  
40  
41  
42  
43  
44  
45  
46  
47  
48  
49  
50  
51  
52  
53  
54  
55  
56  
57  
58  
59  
60  
61  
62  
63  
64  
65

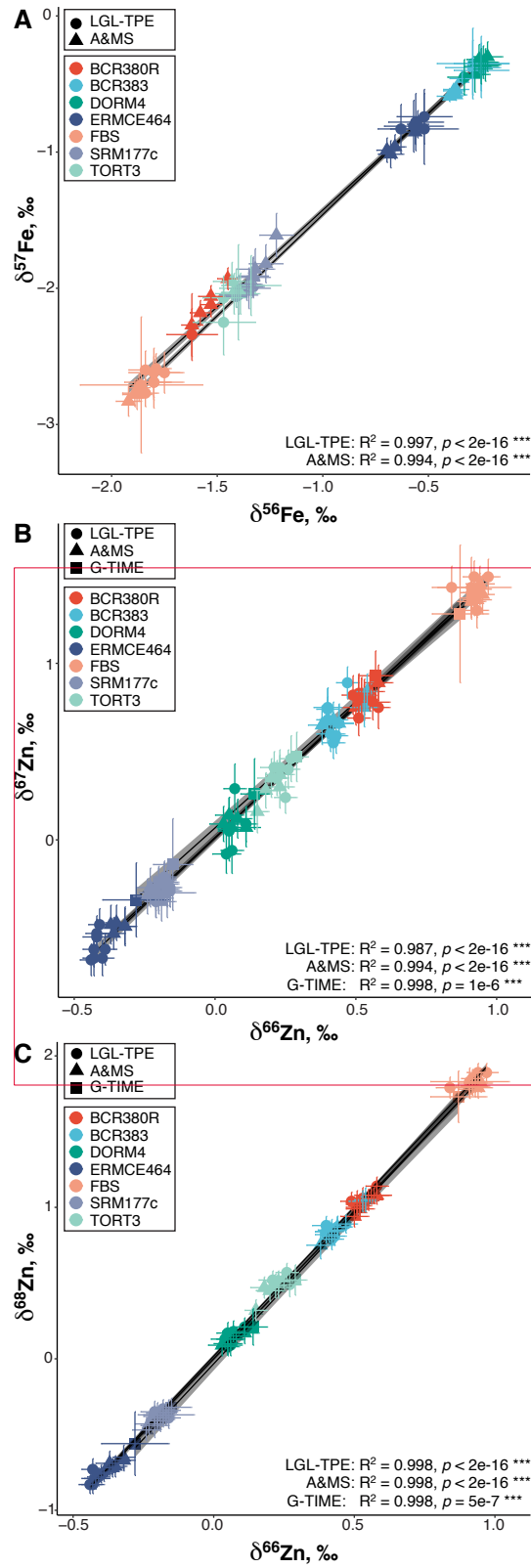


FIGURE 3

1  
2  
3  
4  
5  
6  
7  
8  
9  
10  
11  
12  
13  
14  
15  
16  
17  
18  
19  
20  
21  
22  
23  
24  
25  
26  
27  
28  
29  
30  
31  
32  
33  
34  
35  
36  
37  
38  
39  
40  
41  
42  
43  
44  
45  
46  
47  
48  
49  
50  
51  
52  
53  
54  
55  
56  
57  
58  
59  
60  
61  
62  
63  
64  
65

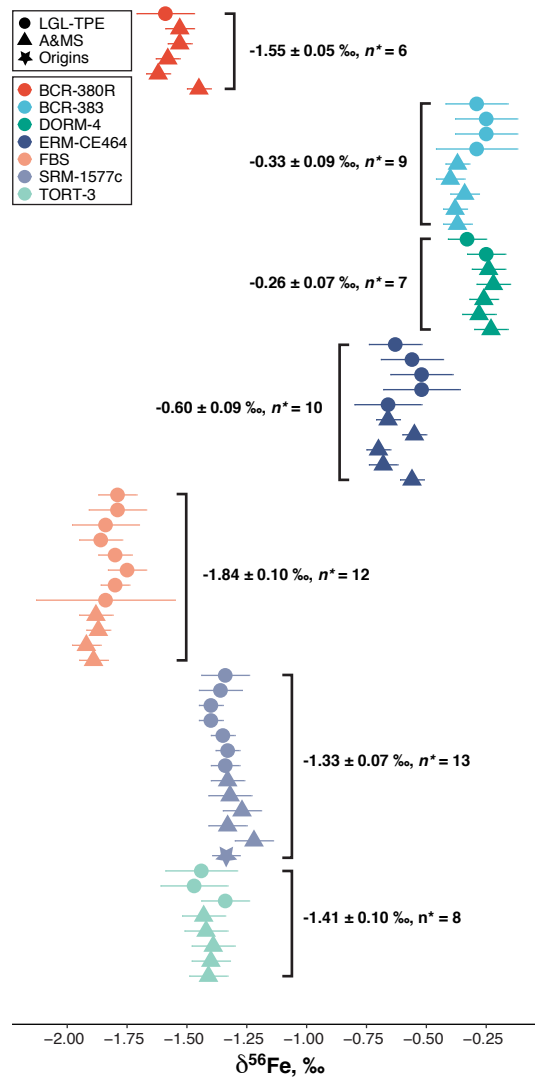


FIGURE 4

1  
2  
3  
4  
5  
6  
7  
8  
9  
10  
11  
12  
13  
14  
15  
16  
17  
18  
19  
20  
21  
22  
23  
24  
25  
26  
27  
28  
29  
30  
31  
32  
33  
34  
35  
36  
37  
38  
39  
40  
41  
42  
43  
44  
45  
46  
47  
48  
49  
50  
51  
52  
53  
54  
55  
56  
57  
58  
59  
60  
61  
62  
63  
64  
65

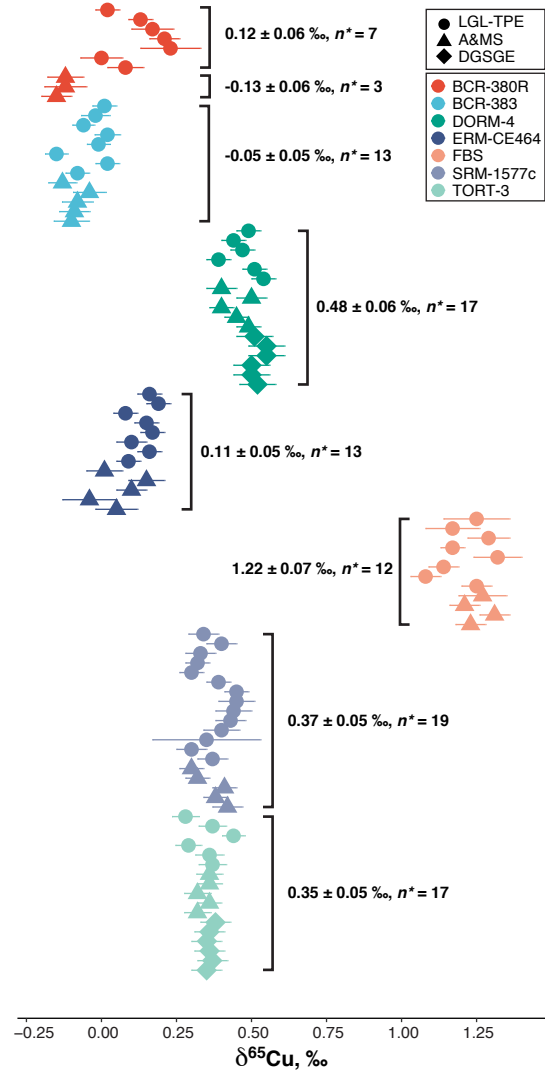


FIGURE 5

1  
2  
3  
4  
5  
6  
7  
8  
9  
10  
11  
12  
13  
14  
15  
16  
17  
18  
19  
20  
21  
22  
23  
24  
25  
26  
27  
28  
29  
30  
31  
32  
33  
34  
35  
36  
37  
38  
39  
40  
41  
42  
43  
44  
45  
46  
47  
48  
49  
50  
51  
52  
53  
54  
55  
56  
57  
58  
59  
60  
61  
62  
63  
64  
65

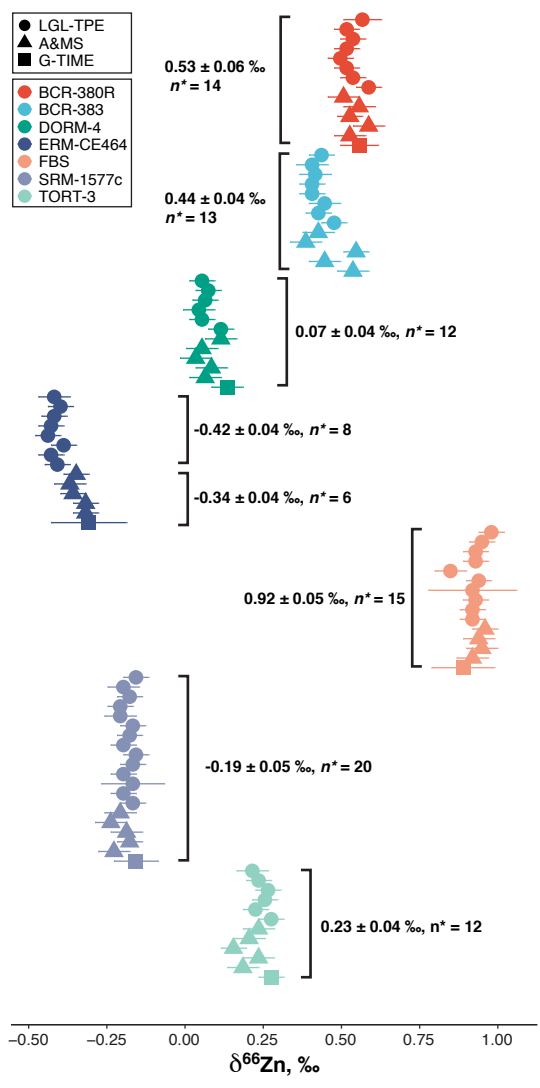


FIGURE 6

Lab	LGL-TPE		A&MS	G-TIME
<b>Element</b>	Fe	Cu, Zn	Cu, Fe, Zn	Zn
<b>Column</b>	Bio Rad	Quartz	Bio Rad	Bio-Rad
<b>Resin</b>	2 mL AG 1-X8	1.8 mL AG MP-1	1 mL AG MP-1	2 mL AG 1-X8
<b>Matrix</b>	8 mL HCl (6M)	10 mL HCl (7 M) + H <sub>2</sub> O <sub>2</sub> (0.001%)	3 mL HCl (8 M) + H <sub>2</sub> O <sub>2</sub> (0.001%)	4 mL HCl (6M) + H <sub>2</sub> O <sub>2</sub> (0.001%)
<b>Cu elution</b>		20 mL HCl (7 M) + H <sub>2</sub> O <sub>2</sub> (0.001%)	9 mL HCl (5 M) + H <sub>2</sub> O <sub>2</sub> (0.001%)	
<b>Fe elution</b>	10 mL HNO <sub>3</sub> (0.5 M)	10 mL HCl (2 M) + H <sub>2</sub> O <sub>2</sub> (0.001%)	7 mL HCl (0.6 M)	
<b>Zn elution</b>		10 mL HNO <sub>3</sub> (0.5 M)	7 mL HNO <sub>3</sub> (0.7 M)	15 mL HNO <sub>3</sub> (1 M) + HBr (0.1 M)

Table 1

1  
2  
3  
4  
5  
6  
7  
8  
9  
10  
11  
12  
13  
14  
15  
16  
17  
18  
19  
20  
21  
22  
23  
24  
25  
26  
27  
28  
29  
30  
31  
32  
33  
34  
35  
36  
37  
38  
39  
40  
41  
42  
43  
44  
45  
46  
47  
48  
49  
50  
51  
52  
53  
54  
55  
56  
57  
58  
59  
60  
61  
62  
63  
64  
65

Lab	LGL-TPE		A&MS			G-TIME
<b>Element (+ internal standard)</b>	Fe (+Ni)	Cu (+Zn), Zn (+Cu)	Fe (+Ni)	Cu (+Ni)	Zn (+Cu)	Zn (+Cu)
<b>MC-ICPMS</b>	Neptune	Nu Plasma	Neptune	Neptune	Neptune	Nu Plasma
<b>RF power (W)</b>	1200	1350	1200	1200	1200	1350
<b>Plasma condition</b>	wet, quartz cyclonic/scott double spray chamber	wet, cyclonic spray chamber	wet, cyclonic/scott double spray chamber	wet, cyclonic/scott double spray chamber	wet, cyclonic/scott double spray chamber	wet, cyclonic spray chamber
<b>Sample uptake rate (<math>\mu\text{L min}^{-1}</math>)</b>	100	100	100	100	100	80-100
<b>Coolant Ar flow (<math>\text{L min}^{-1}</math>)</b>	15	13.5	15	15	15	15
<b>Auxiliary Ar flow (<math>\text{L min}^{-1}</math>)</b>	0.7-1.1	1.25	0.75-0.85	0.75-0.85	0.75-0.85	0.90
<b>Nebulizer Ar flow (<math>\text{L min}^{-1}</math>)</b>	0.9-1.1	1	1.03-1.08	1.03-1.08	1.03-1.08	0.86
<b>Mass resolution</b>	4000 (or 10,000)	300	4000 (or 10,000)	4000	4000	300
<b>Sampling cone</b>	Ni Jet, $\phi = 1.1\text{mm}$	Ni	Ni Jet, $\phi = 1.1\text{mm}$	Ni Jet, $\phi = 1.1\text{mm}$	Ni Jet, $\phi = 1.1\text{mm}$	Ni
<b>Skimmer cone</b>	Ni H-type, $\phi = 0.8\text{mm}$	Ni H-type	Ni H-type, $\phi = 0.8\text{mm}$	Ni H-type, $\phi = 0.8\text{mm}$	Ni H-type, $\phi = 0.8\text{mm}$	Ni WA6
<b>Cup configuration</b>	H3: $^{62}\text{Ni}$ ; H1: $^{60}\text{Ni}$ ; L1: $^{57}\text{Fe}$ ; L2: $^{56}\text{Fe}$ ; L4: $^{54}\text{Fe}$	H5: $^{69}\text{Ga}$ ; H4: $^{68}\text{Zn}$ ; H3: 67.5; H2: $^{67}\text{Zn}$ ; Ax: $^{66}\text{Zn}$ ; L1: 65.5; L2: $^{65}\text{Cu}$ ; L3: $^{64}\text{Zn}$ ; L4: $^{63}\text{Cu}$ ; L5 0.3 ppm $\sim 7\text{ V Cu}_T \sim$ 5V $\text{Zn}_T$	H3: $^{62}\text{Ni}$ ; H1: $^{60}\text{Ni}$ ; Ax: $^{58}(\text{Fe+Ni})$ ; L1: $^{57}\text{Fe}$ ; L2: $^{56}\text{Fe}$ ; L4: $^{54}\text{Fe}$	H3: $^{65}\text{Cu}$ ; H1: $^{63}\text{Cu}$ ; Ax: $^{62}\text{Ni}$ ; L1: $^{61}\text{Ni}$ ; L3: $^{60}\text{Ni}$	H2: $^{68}\text{Zn}$ ; H1: $^{67}\text{Zn}$ ; Ax: $^{66}\text{Zn}$ ; L1: $^{65}\text{Cu}$ ; L2: $^{64}\text{Zn}$ ; L3: $^{63}\text{Cu}$	H6: $^{68}\text{Zn}$ ; H4: $^{67}\text{Zn}$ ; H2: $^{66}\text{Zn}$ ; Ax: $^{65}\text{Cu}$ ; L2: $^{64}\text{Zn}$ ; L4: $^{63}\text{Cu}$ ; L5: $^{62}\text{Ni}$
<b>Sensitivity</b>	1 ppm $\sim 11.5\text{ V Fe}_T$		0.3 ppm $\sim 15\text{V}$	0.2 ppm $\sim 15\text{V}$	0.2 ppm $\sim 2.5\text{V}$	0.5 ppm $\sim 7\text{ V Cu}_T$
<b>Blank signal (2% HNO3)</b>	$^{56}\text{Fe} \sim 10\text{ mV}$	$^{63}\text{Cu} \sim 0.1\text{ mV}$	<0.01%	<0.01%	<0.05%	$^{64}\text{Zn} \sim 0.5\text{ mV}$
<b>Integration time (s)</b>	10	10	4.194	4.194	4.194	10
<b>Cycles</b>	30	30	45	45	45	60

Table 2

1  
2  
3  
4  
5  
6  
7  
8  
9  
10  
11  
12  
13  
14  
15  
16  
17  
18  
19  
20  
21  
22  
23  
24  
25  
26  
27  
28  
29  
30  
31  
32  
33  
34  
35  
36  
37  
38  
39  
40  
41  
42  
43  
44  
45  
46  
47  
48  
49  
50  
51  
52  
53  
54  
55  
56  
57  
58  
59  
60  
61  
62  
63  
64  
65

Lab			LGL-TPE	A&MS	G-TIME
$\delta^{57}\text{Fe}$ vs	Measured	Intercept	0.027 ( $\pm$ 0.019)	-0.003 ( $\pm$ 0.021)	
		Slope ( $\beta$ )	1.486 ( $\pm$ 0.015)	1.422 ( $\pm$ 0.018)	
$\delta^{56}\text{Fe}$	Theoretical $\beta$	Equilibrium	1.475		
		Kinetic	1.488		
$\delta^{67}\text{Zn}$ vs	Measured	Intercept	0.010 ( $\pm$ 0.011)	0.013 ( $\pm$ 0.008)	0.067 ( $\pm$ 0.014)
		Slope ( $\beta$ )	1.515 ( $\pm$ 0.023)	1.484 ( $\pm$ 0.019)	1.427 ( $\pm$ 0.031)
$\delta^{66}\text{Zn}$	Theoretical $\beta$	Equilibrium	1.479		
		Kinetic	1.490		
$\delta^{68}\text{Zn}$ vs	Measured	Intercept	0.018 ( $\pm$ 0.006)	0.002 ( $\pm$ 0.007)	-0.033 ( $\pm$ 0.016)
		Slope ( $\beta$ )	1.967 ( $\pm$ 0.012)	1.948 ( $\pm$ 0.016)	1.985 ( $\pm$ 0.034)
$\delta^{66}\text{Zn}$	Theoretical $\beta$	Equilibrium	1.942		
		Kinetic	1.971		

Table 3

1  
2  
3  
4  
5  
6  
7  
8  
9  
10  
11  
12  
13  
14  
15  
16  
17  
18  
19  
20  
21  
22  
23  
24  
25  
26  
27  
28  
29  
30  
31  
32  
33  
34  
35  
36  
37  
38  
39  
40  
41  
42  
43  
44  
45  
46  
47  
48  
49  
50  
51  
52  
53  
54  
55  
56  
57  
58  
59  
60  
61  
62  
63  
64  
65

**Lucie Sauzéat**: investigation, resources, data curation, writing - review & editing; **Marta Costas-Rodríguez**: investigation, resources, data curation, writing - review & editing; **Emmanuelle Albalat**: investigation, resources, data curation, writing - review & editing; **Nadine Mattielli**: investigation, resources, data curation, writing - review & editing; **Frank Vanhaecke**: writing - review & editing, supervision; **Vincent Balter**: conceptualization, formal analysis, data curation, writing original draft, review and editing, supervision, project administration